ELSEVIER

Physicochemical and redox characteristics of particulate matter (PM) emitted from gasoline and diesel passenger cars

Michael D. Geller[a], Leonidas Ntziachristos[a], Athanasios Mamakos[b],
Zissis Samaras[b], Debra A. Schmitz[c], John R. Froines[c], Constantinos Sioutas[a],*

[a]Department of Civil and Environmental Engineering, University of Southern California, 3620 S. Vermont Avenue,
Los Angeles, CA 90089, USA
[b]Laboratory of Applied Thermodynamics, Aristotle University, Thessaloniki 54124, Greece
[c]Center for Occupational and Environmental Health, University of California, Los Angeles, CA 90095, USA

Abstract

Particulate matter (PM) originating from mobile sources has been linked to a myriad of adverse health outcomes, ranging from cancer to cardiopulmonary disease, and an array of environmental problems, including global warming and acid rain. Till date, however, it is not clear which physical characteristics or chemical constituents of PM are significant contributors to the magnitude of the health risk. This study sought to determine the relationship between physical and chemical characteristics of PM while quantitatively measuring samples for redox activity of diesel and gasoline particulate emissions from passenger vehicles typically in use in Europe. The main objective was to relate PM chemistry to the redox activity in relation to vehicle type and driving cycle. Our results showed a high degree of correlation between several PM species, including elemental and organic carbon, low molecular weight polycyclic aromatic hydrocarbons, and trace metals such as lithium, beryllium, nickel and zinc, and the redox activity of PM, as measured by a quantitative chemical assay, the dithiothreitol (DTT) assay. The reduction in PM mass or number emission factors resulting from the various engine configurations, fuel types and/or after-treatment technologies, however, was non-linearly related to the decrease in overall PM redox activity. While the PM mass emission rate from the diesel particle filter (DPF)-equipped vehicle was on average approximately 25 times lower than that of the conventional diesel, the redox potential was only eight times lower, which makes the per mass PM redox potential of the DPF vehicle about three times higher. Thus, a strategy aimed at protecting public health and welfare by reducing total vehicle mass and number emissions may not fully achieve the desired goal of preventing the health consequences of PM exposure. Further, study of the chemical composition and interactions between various chemical species may yield greater insights into the toxicity of the PM content of vehicle exhaust.
© 2006 Elsevier Ltd. All rights reserved.

Keywords: Diesel; Gasoline; Ultrafine particles; Redox activity

1. Introduction

Particulate matter (PM) originating from mobile sources is thought to be responsible for a myriad of adverse health outcomes, ranging from cancer to

*Corresponding author.
  E-mail address: sioutas@usc.edu (C. Sioutas).

cardiopulmonary disease, and environmental problems, from global warming to acid rain (Adler et al., 1994; Dockery et al., 1993; Lanki et al., 2006; Pope et al., 1995). Vehicles have been shown to emit significant particulate mass and numbers in the form of combustion byproducts and debris from mechanical wear (Cyrys et al., 2003; Shi and Harrison, 1999). Exhaust after treatment, such as catalytic converters and diesel particle filters (DPFs), has resulted in significant reductions in the masses of both gaseous and particulate pollutants. However, total particle number emissions have not been equally reduced, with some studies reporting increases in these emissions due to particle nucleation occurring downstream of after treatment devices (Sakurai et al., 2003; Vaaraslahti et al., 2004). Furthermore, Su et al. (2004) recently reported that modern engines emit smaller primary particles than older engines, which may have health implications.

Characterization of vehicular emissions has been attempted mainly by three types of experimental procedures: on-road, tunnel, and dynamometer measurements. While the latter method requires dilution systems that attempt to replicate ambient concentrations, it offers the advantage of controlling for vehicle type, load and use of after treatment technology. Various dynamometer experiments have successfully characterized different types of diesel vehicles under varying loads (Kittelson, 1998; Su et al., 2004). These studies have determined that a significant fraction of diesel PM is semi-volatile with a mode diameter typically smaller than 50 nm (nucleation mode), whereas a non-volatile (refractory) portion, generally in the 50–200 nm range (accumulation mode), constitutes the bulk of PM mass and consists of particles with an elemental carbon core and low vapor pressure hydrocarbons and sulfur compounds adsorbed on their surface (Burtscher, 2005). Particles may be formed during the combustion process and as vapors cool and condense in the exhaust lines, indicating that both engine and ambient conditions control the fraction of semi-volatile diesel PM that is either in the gas or particle phase.

Several studies have investigated the toxicology of PM and co-pollutants emitted from diesel and gasoline engines (Maejima et al., 2001; Seagrave et al., 2001, 2002, 2003) including both in vivo and in vitro approaches. In most of these studies, the vehicle exhaust was treated as a mixture of pollutants without attempting to link specific chemical components or species of the exhaust to the observed health outcomes. McDonald et al. (2004) reported lung toxicity and mutagenicity by using principal component analysis and partial least-squares regression on data from a dynamometer study (Zielinska et al., 2004b). The conclusions indicated that lung inflammation was primarily associated with hopanes and steranes, which are typically used as tracers of vehicular emissions, but not with any particular metal and/or PAH species. Recent in vitro research using ambient PM, however, has demonstrated a link between particle-bound species, such as selected trace elements and various organics, and redox activity, induction of antioxidant markers for oxidative stress, and mitochondrial damage (Li et al., 2003).

The mechanisms of PM-related health effects are still incompletely understood, but a hypothesis under investigation is that many of the adverse health effects may derive from oxidative stress, initiated by the formation of reactive oxygen species (ROS) within affected cells. There is a growing literature on specific health effects in association with cellular oxidative stress including the ability of PM to induce pro-inflammatory effects in the nose, lung and cardiovascular system (Baulig et al., 2003; Donaldson et al., 2001; Li et al., 2003; Sigaud et al., 2005; Squadrito et al., 2001). High levels of ROS cause a change in the redox status of the cell (Schafer et al., 2003), thereby triggering a cascade of events associated with inflammation and, at higher concentrations, apoptosis (Li et al., 2001). Typically, ROS are formed in cells through the reduction of oxygen by biological reducing agents such as NADH and NADPH, with the catalytic assistance of electron transfer enzymes and redox-active chemical species such as redox-active organic chemicals and metals (Dellinger et al., 2001; Squadrito et al., 2001), and toxicity involving both types of agents has been demonstrated (Veronesi et al., 1999). PM has been shown to participate in these electron transfer reactions (Baulig et al., 2003; Li et al., 2003; Sigaud et al., 2005; Squadrito et al., 2001; Vogl and Elstner, 1989).

The objective of this study is to relate PM chemistry to chemical assays that quantitatively measure reactive oxygen formation (ROS) and are a measure of redox activity with respect to vehicle type and driving cycle. This goal was accomplished by simultaneously collecting filter samples from vehicles for determination of particle physical and chemical characteristics and chemical assays for

redox activity. The study was limited to typical diesel and gasoline passenger vehicles currently in use in Europe. While this study is by no means comprehensive, due to the availability of limited vehicle types, it is the first study of its kind to attempt a correlation between chemical composition with redox activity of PM emitted by passenger vehicles.

2. Methods

2.1. Testing facility

Tests were conducted at the dynamometer facility in the Laboratory of Applied Thermodynamics (LAT) at Aristotle University in Thessaloniki, Greece. The vehicle exhaust was primarily diluted and conditioned according to the constant volume sampling (CVS) procedure. Exhaust was transported to the tunnel through an insulated 6 m long corrugated stainless steel tube, and it was introduced along the tunnel axis near an orifice plate, ensuring rapid mixing with the dilution air. A positive displacement pump controlled the nominal flow rate, $500 \, m^3 \, h^{-1}$, of dilute exhaust gas through the tunnel. In some tests, the HEPA filter was removed from the tunnel inlet to observe the effect of background aerosol to the particle samples collected.

2.2. Test vehicles, fuels, and lubricants

The vehicle sample set included three passenger cars. The first vehicle was a 1.91 Euro 3 diesel (Renault Laguna 1.9 dCi) retrofitted with a catalyzed DPF (NGK SiC 300 cpsi), which replaced a main oxidation catalyst with which the vehicle was originally equipped. The catalyzed DPF was nearly new and aged 10, 000 km. The second vehicle tested was a Euro 3 port fuel injection spark ignition vehicle (Peugeot 406), and the last one was a new Euro 4 compliant diesel passenger car (Honda Accord 2.2 i-CTDi) equipped with a three-stage oxidation after treatment system. Table 1 lists the characteristics of the different vehicles, including their model year and total mileage.

The two diesel vehicles operated on diesel fuel fulfilling the specifications of the latest 2003/17/EC directive and had a sulfur content of 8 ppm wt. The gasoline vehicle used a fuel grade, which fulfilled the requirements of the same Directive and had a sulfur content of less than 50 ppm wt. The lubricant oils used were of a grade recommended by the manufacturer but of unknown composition. The Euro 4 diesel operated on run-in lubrication oil, which is expected to contain a relatively higher metal content than typical lubricants.

2.3. Vehicle test cycles

The vehicles were driven on a chassis dynamometer under both transient and steady-state operation. The cycles employed were the New European Driving Cycle (NEDC), the urban part of the NEDC (UDC) and the Artemis Road cycle. The latter is representative of road driving conditions commonly encountered in Europe and has been developed in the framework of the Artemis project (Andre, 2004). In addition, the vehicles were tested at a constant cruising speed of 90 km per hour (kph) under road load in order to sample under typical freeway cruising conditions.

Before each measurement, the vehicle and the CVS tunnel were conditioned by driving the vehicle over a UDC or a NEDC followed by a period of steady speed cruising at 90 kph. This also provided the means of checking the status of the FPS diluter (described below). A more intense conditioning of the CVS tunnel (2 × Artemis Road and 90 kph steady speed) was applied before the first test of the gasoline vehicle in order to minimize the possibility of contamination from the previously tested DPF-diesel vehicle.

2.4. Emissions sampling

A Dekati Fine Particle Sampler (FPS Model FPS-4000, Dekati, Ltd., Tampere, Finland) sampled and further diluted a sample from the CVS tunnel with conditioned air. Depending on the emission levels of the vehicles tested, one or two additional ejector-type diluters have been used in order to bring the aerosol concentrations within the measuring range of each instrument. The dilution ratio of the FPS was monitored daily over the 90 kph tests, using CO_2 as a trace gas. The dilution ratio of the ejector diluters was determined by trace gas calibration in separate measurements (Giechaskiel et al., 2004).

The instruments employed for the physical characterization of the vehicle particulate emissions are summarized below. A Condensation Particle Counter (CPC Model 3010, TSI, Inc., St. Paul, Minnesota, USA) monitored the number of concentration of the total particle population (50%

Table 1
Vehicle specifications and test sequence

Fuel	"Euro" level (model year)	Model (mileage)	OEM after-treatment	After-treatment during test	Conditioning	Test (cycle or steady state)
Diesel	Euro 3 (2001)	Renault Laguna 1.9 dCi (60 Mm)	Oxidation pre-catalyst and main under-floor catalyst	Oxidation pre-catalyst and catalyzed ceramic diesel particle filter	1 × UDC and 90 kph at 0.5 h	8 × Artemis Road
					1 × UDC and 90 kph at 0.5 h	90 kph at 50 min
						8 × Artemis Road
					2 × Artemis Road and 90 kph at 1 h	90 kph at 60 min
Gasoline	Euro 3 (2001)	Peugeot 406 1.6i (120 Mm)	Three-way catalyst			4 × Artemis Road
					1 × NEDC and 90 kph at 1 h	90 kph at 45 min
						3 × Artemis Road
Diesel	Euro 4 (2005)	Honda Accord 2.2 i-CTDi (5 Mm)	Oxidation pre-catalyst and two-stage oxidation under-floor catalyst		1 × NEDC and 90 kph at 1 h	Artemis Road
						90 kph at 15 min 3 × Artemis Road 90 kph at 15 min

Particulate matter from each individual test is collected on a Teflon, a quartz and a TFE-coated glass-fiber filter. The "Euro" level corresponds to vehicle certification with OEM after-treatment.

cutpoint ~10 nm) in real time. A Scanning Mobility Particle Sizer (SMPS Model 3936L, TSI, Inc., St. Paul, Minnesota, USA) was employed instead of the CPC during the steady-state runs in order to measure the number weighted size distributions between ~10 and 400 nm. The sheath-air and monodisperse flow rates were set at 6 and 0.6 lpm, respectively. Dekati's Diffusion Charger (DDC), a prototype diffusion charger calibrated by LAT, as described by Ntziachristos et al. (2004), measured the active surface area of airborne particles in real time. An Electrical Low Pressure Impactor (ELPI, Dekati, Ltd., Tampere, Finland) monitored the number weighted (aerodynamic) size distribution in real time. The ELPI operated with oil-soaked sintered plates and a filter stage that extended the lower cutpoint to ~7 nm. A thermodenuder (Model ELA-230, Dekati, Ltd., Tampere, Finland) was set at a fixed temperature of 250 °C, which has been shown to adequately remove most of the volatile material. Thus, only solid particles will be measured downstream of the thermodenuder.

During transient tests, the ELPI was located downstream of the thermodenuder and was therefore measured the solid particle population. The remaining instruments monitored the total particle population. Two additional configurations were employed throughout the steady-state tests, with the SMPS and the ELPI sampling simultaneously upstream and downstream of the thermodenuder, which allowed for measurement of the solid and total particle concentrations. A schematic of the setup employed in the measurements is shown in Fig. 1.

A number of filters of different size and material were used in parallel to collect PM samples for chemical and toxicological analysis. Gravimetric mass and metal species concentrations were determined from samples collected on 47 mm Teflon filters (2 μm pore, Pall Corp.); 47 mm quartz filters (Pall Corp., East Hill, NY, USA) were also used to collect particles for analysis of elemental and organic carbon (EC/OC) as well as polycyclic aromatic hydrocarbons (PAH). Quartz filters were pre-baked at 550 °C for 8 h and stored in baked aluminum foil-lined containers prior to deployment. Sampling flow rates were set at 10 lpm and were controlled by mass flow meters. Mass concentrations were determined by measuring the net filter weight gain after sampling and equilibration in a

Fig. 1. Schematic of the experimental setup employed over the transient tests. Two additional configurations were employed over the 90 kph tests, with the SMPS and the ELPI sampling simultaneously either upstream or downstream of the thermodenuder.

temperature and humidity controlled room. EC/OC concentrations were measured by thermal optical transmittance (Birch and Cary, 1996), and PAHs were quantified by HPLC with selective fluorescence detection (Eiguren-Fernandez and Miguel, 2003). Metals were determined via ICP-MS as described by Lough et al. (2005). TFE-coated glass-fiber filters (Pallflex Fiberfilm T60A20-20 × 25.4 cm, Pall Corp.), sampling at a flow of 380 lpm, were used to collect mass for in vitro toxicology assays. These filters were washed with a solution of dichloromethane (DCM) and methanol three times and dried prior to deployment. Such coated filters have been used to collect particles previously (Jang and Kamens, 2001) and were chosen to minimize the organic vapor adsorption artifacts that are often associated with quartz fiber filters. In order to collect sufficient mass on each filter, a variable number of test cycles were run with each vehicle, depending on its emission levels.

2.5. Dithiothreitol (DTT) assay

This assay provides a measure of the overall redox activity of the sample based on its ability to catalyze electron transfer between DTT and oxygen in a simple chemical system (Cho et al., 2005). The electron transfer is monitored by the rate at which DTT is consumed under a standardized set of conditions and the rate is proportional to the concentration of the catalytically active redox-active species in the sample. This assay has been applied to ambient size-fractionated PM samples and the activity is associated with the ability to induce hemoxygenase-1 expression (Li et al., 2003). This assay was used in our experiments to measure the redox potential of PM collected from different vehicles and test configurations. Particles collected on the TFE-coated glass-fiber filters were sonicated in Milli-Q water for 20 min. The filters were removed and the aqueous particle suspension was used in the assay. The assay is described in detail by Cho et al. (2005). In brief, the PM samples are incubated with DTT (100 μM) in phosphate buffer (0.1 M, pH 7.4) for varying times from 0 to 30 min, and the reaction quenched at preset times by addition of 10% trichloroacetic acid. An aliquot of the quenched mixture is then transferred to a tube containing Tris HCl (0.4 M, pH 8.9), EDTA (20 mM) and 5,5′-dithiobis-2-nitrobenzoic acid (DTNB, 0.25 mM). The concentration of the remaining DTT is determined from the concentra-

tion of the 5-mercapto-2-nitrobenzoic acid formed by its absorption at 412 nm. The DTT consumed is determined from the difference between the mercaptobenzoate formed by the blank and that formed by the sample. The data collected at the multiple time points are used to determine the rate of DTT consumption which is normalized to the quantity of PM used in the incubation mixture.

2.6. Calculations

All real-time CPC, DDC and ELPI recordings were aligned with the recordings of speed and CVS flow. Then, the total particle number (ELPI–CPC) and surface area (DDC) emitted over the whole cycle were multiplied with the total flow in the CVS tunnel (under normal conditions) and divided by the corresponding distance covered. The CPC results have been corrected for coincidence effects. In general, this correction was small (<8%) since the measured concentrations were effectively kept below 10,000 particles cm^{-3}.

ELPI concentrations were determined considering only the first seven impactor stages (not including the filter stage). The data reduction (which also considers collection due to diffusion and space-image charge) requires an assumption for the particle effective density. The effective particle density as a function of size was derived by combining the ELPI and the SMPS results (Virtanen et al., 2004). This information was available for the steady-state tests of all vehicles, except the gasoline-fuelled car which emits particle numbers at the ELPI noise level. The calculated effective densities were then used to calculate ELPI results also during transient tests. The particle effective density (and morphology) depends on the operating conditions; hence, the transfer of density values from steady state to transient tests is associated with some uncertainty. However, this approach should be considered more realistic than that of unit density spherical particles. The latter has been used only for the gasoline car, because particles emitted from these vehicles typically do not contain a large number of fractal agglomerates but consist mostly of spherical condensates of organic material with density on the order of 0.8–1.2 g cm^{-3} (Geller et al., 2006). Finally, the solid particle losses inside the thermodenuder were also accounted for according to Dekati, Ltd. (Dekati, 2001). For the flow rate used in the measurements (∼10 lpm), the losses are almost constant and equal to 23% from the upper

size range down to 60 nm and increase with decreasing diameter, reaching 34% at 10 nm.

3. Results and discussion

3.1. PM emissions

Table 2 displays the PM mass and chemical species emissions (in mg km^{-1} and µg km^{-1} for selected PAHs) for each test, separated by vehicle type and type of after treatment. It is evident from the data listed in this table that the diesel vehicle retrofitted with a catalyzed DPF gave the lowest PM matter emissions. The PM emissions ranged between 0.88 and 1.02 mg km^{-1} over the Artemis Road and between 0.32 and 0.56 mg km^{-1} over the steady states. The PM mass emissions of the gasoline vehicle under road driving conditions were determined to be 5.5 and 6 mg km^{-1}. During 90 kph constant speed cruising, the gasoline vehicle emitted extremely low particulate emissions (e.g., 0.41 mg km^{-1}), which were comparable to those obtained from the DPF vehicle during steady state. The conventional diesel vehicle (Honda Accord) emitted the highest amounts of PM, averaging 24.9 ± 5.9 mg km^{-1} of PM over the transient tests and a slightly lower rate of 14.1 mg km^{-1} during the constant speed cycle. The above emission rates indicate that the various vehicles and testing configurations were well within the range of typical emission data for gasoline and diesel passenger

vehicles operating with and without after-treatment technologies of other studies (Zielinska et al., 2004b), which supports the generalizability of our findings regarding PM properties from these vehicles.

The particle number and surface area emission rates of the different vehicles driven over the Artemis Road tests are summarized in Fig. 2A. To accommodate for the different emission levels of the vehicles, the results are plotted in logarithmic scale. Generally, emissions rates by number and surface demonstrated similar trends as the PM mass emissions. The diesel vehicle was the highest particle number emitter, with emissions ranging between 5.15 and 5.20 × 10^{13} particles km^{-1} and between 3.63 and 4.08 m^2 km^{-1} for number and surface area, respectively. The particle numbers emitted by the gasoline vehicle varied between 2.5 and 3.6 × 10^{12} particles km^{-1}, which are about an order of magnitude lower than the conventional diesel. The active surface area of the total particle population measured between 0.14 and 0.22 m^2 km^{-1}. It is also noteworthy that the removal of the CVS filter did not seem to affect the recorded particle concentration. It was hypothesized that the addition of particle-laden air could enhance nucleation by providing possible surfaces for vapor adsorption. The lowest particle number emissions were those of the DPF-equipped vehicle, ranging from 3.2 to 5.1 × 10^{11} particles km^{-1}, thus, almost 100-fold lower than those of the conventional diesel passenger vehicle, and the active

Table 2
Emission rates of PM mass (mg km^{-1}), elemental and organic carbon and selected PAH species (ng km^{-1})

Component	Diesel transient	Diesel SS[a]	Gasoline	Gasoline SS[a]	Cat DPF transient	Cat DPF SS[a]
Mass (mg km^{-1})	25 ± 6	14	5.8 ± 0.3	0.4	1.0 ± 0.1	0.4 ± 0.1
Elemental carbon (EC)	12911 ± 335	7095	473 ± 134	13	137 ± 66	67 ± 40
Organic carbon (OC)	4967 ± 1687	5751	1462 ± 491	375	482 ± 45	230 ± 78
Naphthalene	217 ± 73	201	15 ± 5	1.9	1.7 ± 1.4	ND[b]
Phenanthrene	285 ± 88	61	39 ± 16	3.4	7.3 ± 1.7	4.0 ± 0.2
Anthracene	7.6 ± 2.4	5.1	5.4 ± 1.9	0.4	0.3 ± 0.3	ND[b]
Fluoranthene	12 ± 5.4	ND[b]	43 ± 12	5.3	12 ± 1.7	5.8 ± 3.2
Pyrene	161 ± 21	107	48 ± 12	5.4	26 ± 3.2	9.6 ± 6.6
Benz(a)anthracene	5.0 ± 0.8	1.2	23 ± 4.2	17.0	13 ± 5.0	6.4 ± 1.0
Chrysene	6.1 ± 0.4	1.7	31 ± 4.4	27.7	17 ± 4.3	11 ± 1.2
Benzo(b)fluoranthene	0.7 ± 0.2	ND	6.7 ± 0.5	1.2	7.0 ± 5.4	1.8 ± 0.8
Benzo(k)fluoranthene	ND[b]	ND	1.6 ± 0.4	0.5	ND	ND
Benzo(a)pyrene	ND	ND	4.2 ± 0.4	0.3	0.2 ± 0.2	ND
Benzo(g)perylene	ND	ND	7.7 ± 2.9	0.3	ND	ND

Standard deviations are presented when multiple tests have been averaged.
[a] SS = steady state.
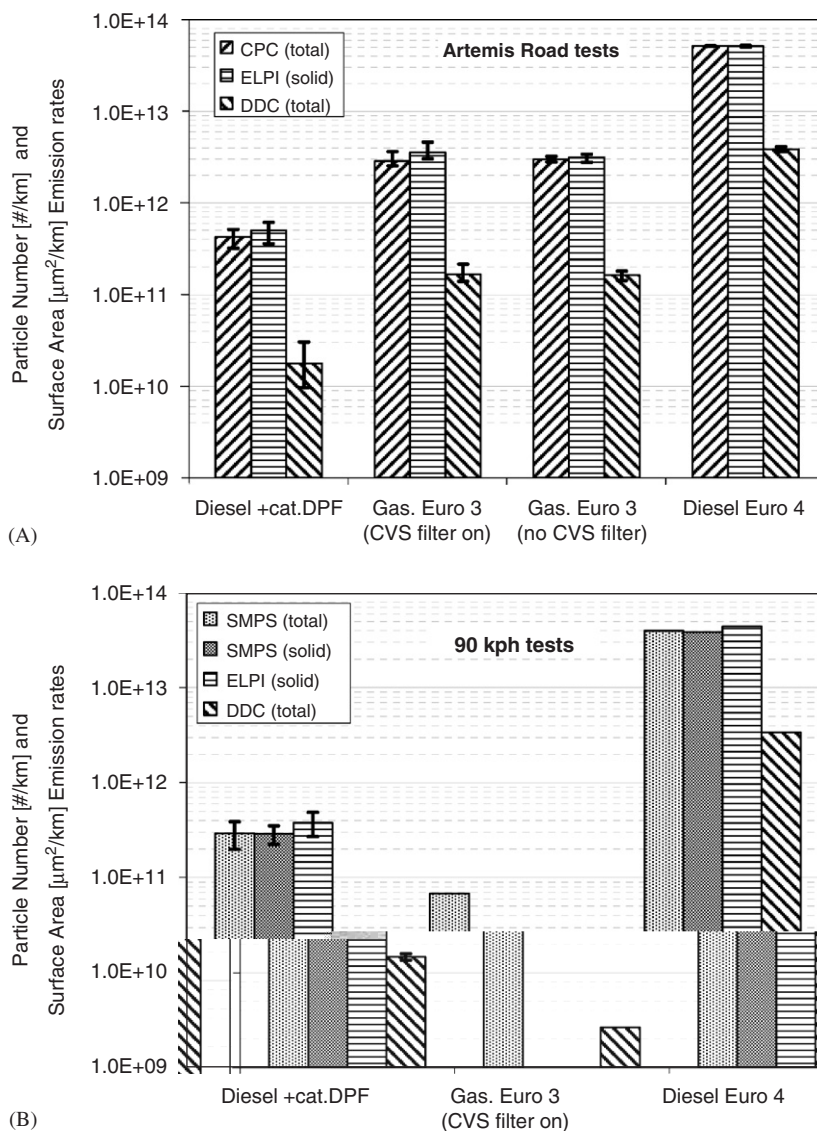[b] ND: below the limit of detection.

Fig. 2. (A) Cycle average particle emissions of the various vehicles tested. (B) Particle emissions of the various vehicles tested over the 90 kph tests. The bars correspond to the grand average of all tests conducted while the error bars indicate the minimum–maximum results obtained.

surface area of the emitted particles varied between 97 and $305\,cm^2\,km^{-1}$.

The number concentration of solid particles (those not removed by the thermodenuder operating at $250\,°C$) was at same level with the number concentration of the total particle population for all vehicles tested. Although this comparison is affected from the assumptions inherent in the ELPI calculations (i.e., uncertainties in the effective density value), the results indicate that there was no significant formation of "secondary" volatile particles. It should be noted that this result by no means

implies that these vehicles do not emit semi-volatile PM, a fact already demonstrated by several other studies mentioned earlier, but they did not emit them at the *specific experimental conditions* under which our tests were conducted.

The particle number and surface area emission rates from the 90 kph tests are summarized in Fig. 2B. With respect to the diesel vehicles, the DDC and the ELPI results were at the same levels as those measured over the Artemis Road tests (within 30%). The somehow reduced SMPS concentration, compared to the ELPI could
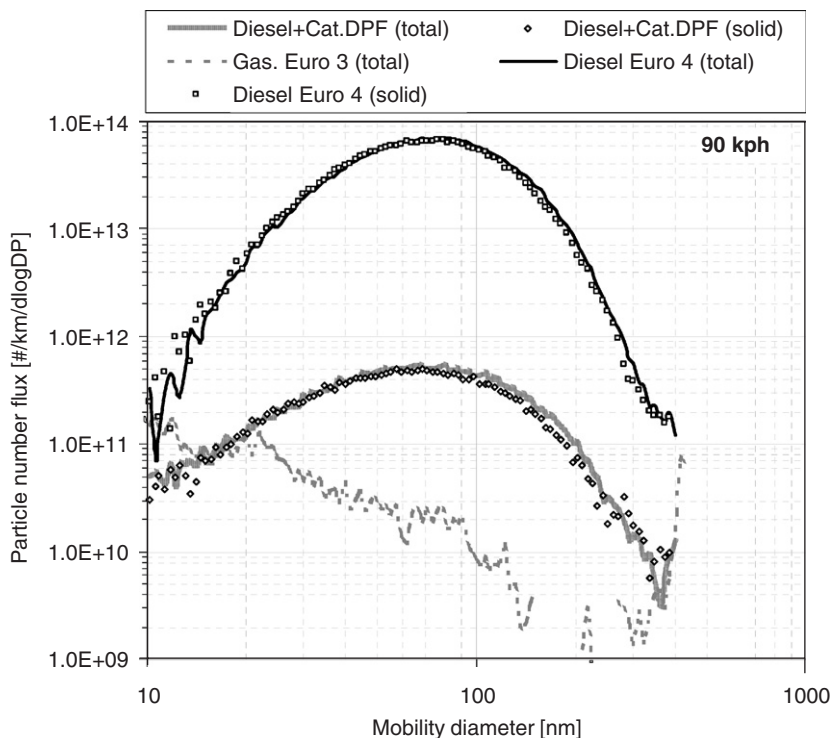
Fig. 3. Number weighted size distributions as measured with the SMPS over the 90 kph tests. The presented distributions correspond to the average of all SMPS scans taken during each 90 kph test.

be due to particles losses in the SMPS (Burtscher, 2005).

Contrary to the conventional diesel vehicle, for which the PM number and surface area concentrations were slightly lower in the steady-state test, significant differences between transient and steady-state cycles were observed for the gasoline vehicle. Under steady-state conditions, the gasoline vehicle emitted 3.8×10^8 particles km^{-1} and 26 cm^2 km^{-1}, which are about two orders of magnitude lower than the transient tests. The emission levels were in fact lower than the limit of detection of the ELPI, which explains why there are no data available for that instrument in Fig. 2B. The low emission levels over steady-state tests are due to the accurate control of the stoichiometric air-to-fuel ratio at constant speed driving. In transient tests, frequent excursions from stoichiometry during accelerations lead to an overall increase of the average emission level.

Due to the variable emission levels during transient tests, measurements of the particle size distributions with the SMPS were only possible during steady-state runs. The number weighted size distributions of both total and solid particle

populations are shown in Fig. 3. A lognormal distribution was obtained for all diesel vehicles. Moreover, similar distributions were obtained with and without thermal conditioning of the aerosol, indicating again the absence of significant numbers of non-solid particles. The aerosol geometric mean diameters were between 60 and 70 nm for the three diesel vehicle configurations. In contrast, the particle size distributions of the gasoline vehicle were distinctly different, with the number concentrations monotonically decreasing with particle size and a geometric mean diameter of $\sim$25 nm.

3.2. Elemental and organic carbon and PAH emission factors

Emission factors for individual elements and compounds are presented in Tables 2 and 3. Table 2 summarizes emission factors for elemental and organic carbon as well as PAHs. Generally, the diesel vehicle emitted the highest amounts of EC per kilometer, with the transient and steady-state cycles ranked first and second in emission rates. In contrast to the EC data, the OC emissions during steady-state operation of the diesel vehicle were

quite similar, but still the highest of all vehicles tested. Similar results for EC and OC emission factors were reported by Durbin et al. (2000) and Zielinska et al. (2004b). The DPF-diesel vehicle demonstrated the lowest EC-OC carbon mass emissions due to the effective removal of solid particles by the catalyzed DPF. The EC levels of the DPF-equipped vehicle are about 1% of those of the conventional diesel vehicle, whereas the OC emission rates are on average 11% of that vehicle. These results support the argument made in previous studies that organic carbon is often not reduced as effectively as elemental carbon, possibly because a significant fraction of OC may exist as vapors that can condense downstream of the DPF (Burtscher, 2005; Mayer et al., 1999). The gasoline vehicle emitted 97% less EC and 69% less OC than the diesel vehicle, consistent with similar results previously reported (Zielinska et al., 2004b).

Although both EC and OC constituted the majority of the emissions of the engines tested here, the ratio of OC to EC varied with vehicle type. EC dominated OC for the diesel vehicle, whereas OC dominated EC for the gasoline vehicle and the DPF-diesel vehicle. The ratios of OC to EC were 0.38 and 0.81 for transient and steady-state driving of the diesel vehicle, respectively. The catalyzed DPF added to the DPF-diesel vehicle removed EC and OC emissions such that they were 99% and 90% less than the diesel vehicle. In fact, the OC-EC ratios of the DPF-diesel vehicle were 3.52 and 3.44 for transient and steady-state driving, respectively, which closely resemble the same ratio for the gasoline vehicle (3.09).

Interesting comparisons can be drawn between the PAH emissions from different vehicle configurations. With the exception of naphthalene, for which the steady state and transient cycle levels were similar, nearly all measured PAH were reduced by 40–75% when the diesel vehicle operated at steady speed versus varying load. Similarly, the PAH concentrations of the DPF-diesel vehicle in the steady-state cycle were lower than those of the transient by 40–60%. By contrast, the steady-state cycle PAH for the gasoline vehicle were more than 90% lower than those of the transient cycle, except for chrysene and benz(a)anthracene, for which the levels were quite similar but still lower than the transient cycle. The DPF-diesel vehicle demonstrated overall greatly reduced low molecular weight PAH, but it emitted somewhat higher concentrations of high molecular weight PAH when contrasted with the diesel vehicle. During their respective transient runs, naphthalene, phenanthrene, anthracene, and pyrene were more than 95% lower in the exhaust of the DPF diesel vehicle, whereas benz(a)anthracene, chrysene, and benzo(b)-fluoranthene were between two- to three-fold higher. Fluoranthene emissions were nearly equivalent. Differences in the PAH emission between these two vehicles may be due to the fact that the Euro 4 vehicle has a 3-stage oxidation after-treatment system with a total capacity of 3.2 l and a high precious metal loading (up to $90 \, \text{g ft}^{-3}$), whereas the Euro 3 vehicle included a small closed coupled catalyst ($\sim$0.5 l) and a 2-l catalyzed DPF with a precious metal loading of $\sim$40 g ft^{-3}. This means that the oxidation activity of the Euro 4 is much stronger than that of the Euro 3, resulting in a more effective oxidation of high molecular weight PAHs accomplished by that vehicle.

Similar trends were observed for the gasoline vehicle's emission profile (Table 2), which also demonstrated greater emission of the heavier PAH, a result that is consistent with previous studies, reporting similar differences in PAH profiles between diesel and gasoline vehicles (Gross et al., 2000; Marr et al., 1999; Miguel et al., 1998; Venkataraman et al., 1994; Zielinska et al., 2004a). The high molecular weight PAH emission by gasoline vehicles has been attributed to the fact that lube oil in gasoline vehicles absorbs and concentrates PAH (including heavy, particle-associated PAH) that are formed during combustion, and as a result, the PAH from these vehicles were at least in part emitted as a component of unburned lubrication oil. In contrast, the PAH profile of the diesel vehicles is similar to the PAH content of their fuel (Zielinska et al., 2004b).

3.3. Elemental composition

Individual trace element and metal emission factors are presented in Table 3. Crustal metals are separated at the top of the table because these elements make up the bulk of the metal mass composition of diesel fuel and diesel emissions (Wang et al., 2003). This holds for the results of the vehicles tested here with a few exceptions. The diesel vehicle, in both steady-state and transient testing, emitted Zn at a rate comparable to the crustal metals. The emission profile of the gasoline vehicle was similar to those of the diesel vehicles in that the crustal metals were among the highest

Table 3
Emission factors of selected trace elements (ng km^{-1})

Element	Diesel transient	Diesel SS	Gasoline transient	Gasoline SS	Cat. DPF transient	Cat. DPF SS
Al	9108 ± 5224	2706	2273 ± 545	252	712 ± 41	270 ± 70
Ca	$69{,}443 \pm 23{,}640$	16,128	$18{,}247 \pm 3044$	2324	2497 ± 931	849 ± 250
Fe	$22{,}910 \pm 21{,}448$	2036	$10{,}266 \pm 9928$	138	3193 ± 297	296 ± 191
K	4672 ± 752	1191	1935 ± 558	117	462 ± 295	180 ± 20
Mg	3087 ± 461	997	5183 ± 1706	183	279 ± 98	98 ± 11
Na	7736 ± 1751	1945	2237 ± 1125	321	1043 ± 507	385 ± 67
Ba	583 ± 349	73	331 ± 55	4.8	41 ± 12	6.7 ± 1.0
Be	26 ± 12	23	6.7 ± 1.1	1.5	1.4 ± 0.7	1.7 ± 0.4
Cr	634 ± 354	93	138 ± 6.7	8.6	152 ± 2.8	9.6 ± 6.4
Cu	1944 ± 679	627	1745 ± 1803	16	1166 ± 165	74 ± 46
Li	13 ± 0.2	7.9	3.0 ± 1.4	0.9	0.9 ± 0.2	0.5 ± 0.2
Mn	368 ± 183	76	152 ± 85	3.4	62 ± 33	4.4 ± 0.2
Ni	2310 ± 656	644	107 ± 0.7	21	71 ± 21	3.2 ± 0.9
Pb	793 ± 593	79	237 ± 2.3	11	156 ± 42	16 ± 8.0
S	$23{,}750 \pm 5295$	6713	8705 ± 3375	349	1095 ± 156	513 ± 68
Ti	1036 ± 320	345	118 ± 9.3	24	252 ± 302	59 ± 34
V	28 ± 9.4	11	15 ± 11	1.8	3.7 ± 0.1	1.1 ± 0.4
Zn	$21{,}118 \pm 4422$	5620	4650 ± 1225	198	533 ± 103	73 ± 85

Standard deviations are presented when multiple tests have been averaged.

elemental concentrations present in the exhaust. The concentration of sulfur in each vehicle's exhaust was the highest of the non-metallic elements analyzed, and its relative abundance was very high in each vehicle configuration (between second and fourth out of 18 elements). For the diesel car, the contribution of sulfur in PM is much less than the typical level of ~15% sulfate reported by Kittelson (1998). This is probably due to the negligible sulfur content in the fuel (8 ppm wt) and to the low lubricant consumption of this new vehicle. On the other hand, the relatively high amount of sulfur emitted by the gasoline vehicle (roughly 30% of that emitted by the diesel vehicle) is due to the higher sulfur content of the fuel (~50 ppm wt) and the higher lubricant consumption from this aged vehicle.

Besides iron, barium, magnesium, and copper, which were found in similar (Ba, Fe, Mg) or higher (Cu) amounts in the gasoline vehicle emissions, the conventional diesel vehicle emitted 3–5 times higher amounts per km of most metals and trace elements, a result consistent with the tunnel studies by Geller et al. (2005). The largest difference between the gasoline and diesel vehicles was observed for Ni, whose emission rates were almost 20 times higher in the diesel vehicle. This may be due to the potentially higher metal content of the lubrication oil used in the Euro 4 diesel vehicle, compared to the DPF and the gasoline ones. Compared to the diesel vehicle, the DPF-diesel vehicle released on average about

70–95% lower emissions of metals and trace elements per kilometer driven.

Coefficients of statistical determination (R^2) between the different PM species measured in our testing configurations are shown in Table 4. Considering that the concentrations of trace elements as well as PAH varied by more than one order of magnitude among different vehicle configurations, the degree of correlation between their emission rates was examined by transforming these data into their logarithms. For clarity, in our presentation we only included R^2 values higher than 0.5. R^2 values higher than 0.80 are shown in bold letters. Only species found in measurable quantities for all vehicle configurations were included in this table. Species emitted mostly by the diesel vehicles, such as EC, light PAH (naphthalene, pyrene, phenanthrene), and metals such as Li, Be, Ti, Ni, Zn were very highly correlated, with R^2 exceeding 0.75–0.80. Heavier PAH (fluoranthene, benzo anthracene, chrysene) found mostly in the emission of the gasoline vehicle were also highly correlated. High correlations were also obtained for Fe and Cu, indicating possibly a common origin, as discussed earlier.

We have further attempted a comparison between the sum of the measured chemical species and the gravimetrically determined mass concentrations for each vehicle configuration tested. For the purposes of that comparison, OC was multiplied by a factor

Table 4
Coefficients of statistical determination (R^2) between the log transformed emission factors of chemical PM constituents

	OC	EC	NAP	PHE	ANT	FLT	PYR	BAA	CRY	Li	Be	Na	Mg	Al	S	K	Ca	Ti	V	Cr	Mn	Fe	Ni	Cu	Zn	Ba	Pb
OC	1.00																										
EC	**0.87**	1.00																									
NAP	**0.93**	**0.87**	1.00																								
PHE	0.73	**0.82**	**0.86**	1.00																							
ANT	0.62	0.59	0.60	0.68	1.00																						
FLT						1.00																					
PYR	**0.83**	**0.98**	**0.89**	**0.90**	0.64		1.00																				
BAA						**0.80**		1.00																			
CRY	0.51	0.52				0.79		**0.99**	1.00																		
Li	**0.95**	**0.86**	**0.91**	**0.84**	0.63		**0.85**			1.00																	
Be	**0.95**	**0.84**	**0.98**	**0.87**	0.64		**0.86**			**0.97**	1.00																
Na	0.56	0.50	0.60	0.75			0.55			0.75	0.70	1.00															
Mg					0.67								1.00														
Al	0.75	0.79	**0.86**	**0.98**	0.79		**0.88**			**0.84**	**0.88**	0.70	0.59	1.00													
S	0.71	0.60	0.72	**0.84**	0.79		0.66			**0.83**	**0.83**	0.79	0.71	**0.89**	1.00												
K	0.50		0.67	0.85	0.58		0.58			0.63	0.72	0.75	0.75	**0.86**	**0.84**	1.00											
Ca	0.69	0.64	**0.80**	**0.93**	0.77		0.74			**0.80**	**0.86**	0.75	0.73	**0.96**	**0.95**	**0.94**	1.00										
Ti												0.55						1.00									
V	0.64		0.55	0.63	0.64					0.77	0.69	0.79	0.56	0.68	**0.92**	0.63	0.76		1.00								
Cr																				1.00							
Mn				0.53						0.52	**0.89**	0.50	0.52	0.72	0.71		0.65		0.78		1.00						
Fe																			0.55		0.66	1.00					
Ni	0.75	**0.94**	0.76	0.79		**0.92**			0.50	**0.80**	0.74	0.58		**0.71**	0.52		0.56						1.00				
Cu																					0.70			1.00			
Zn	**0.81**	**0.82**	**0.84**	**0.94**	**0.83**		**0.87**			**0.90**	**0.89**	0.72	0.54	**0.97**	**0.93**	0.77	**0.93**		0.78		0.54			0.74	1.00		
Ba				0.55	0.59					0.59	**0.91**	0.62		**0.80**	**0.80**		0.76		0.71				0.75	0.51	0.60	1.00	
Pb																											1.00

of 1.2 to account for associated hydrogen and other elements that are associated with OC mass (Pierson and Brachaczek, 1983). The concentrations of trace elements were adjusted assuming that they are present in their most commonly found crustal form (Solomon et al., 1989). The sum of chemical species is plotted in Fig. 4 as a function of the gravimetrically determined mass concentration, along with the linear regression between these data. Fig. 4 shows highly correlated data ($R^2 = 0.96$), with the reconstructed mass (sum of chemical species) being on average 0.95 of the measured mass. Considering the uncertainties in the correction factors used in our calculations, this agreement should be considered excellent. This also suggests that the OC concentrations measured in our study are probably not biased by adsorption artifacts, which are quite common when using quartz filters to sample organics (Eatough et al., 1996; Kirchstetter et al., 2001; Turpin et al., 1994). In almost all of our experimental configurations, the sum of chemical species is slightly lower than the total measured mass. One possible explanation for the decreased adsorption of organic vapors during our tests may be that the quartz filters become saturated quite rapidly at the beginning of the sampling cycles, due to the potentially elevated concentrations of organic vapors emitted for the various vehicles. In a previous study in Pittsburgh (Subramanian et al., 2004), an average positive OC artifact of 0.48 (± 0.15) µg of C per cm^2 of quartz filter area was reported, whereas Arhami et al. (2006) reported similar artifact values in the quartz substrates of the Sunset Labs EC-OC monitor, with an average adsorption artifact on quartz filters of 0.98 (± 0.5) µgC cm^{-2}. Assuming to a first approximation that the magnitude of the adsorption artifact on the quartz filters of our study was on the same order to that reported previously, and a 47 mm filtration surface area of 13.5 cm^2, the amount of OC adsorbed in our experiments should be on the order of 10–15 µg C. The amounts of OC collected during our tests in each filter ranged from 65 to 270 µg C, thus, substantially higher than the estimated amount of the adsorbed organic vapor.

3.4. Redox potential of PM from different vehicles and driving configurations

The redox activity of the samples, based on DTT consumption rates, is expressed in nmole min^{-1} km^{-1}, in Table 5. It should be noted that the assay could not be conducted on filters from steady-state runs of the DPF-diesel vehicle and

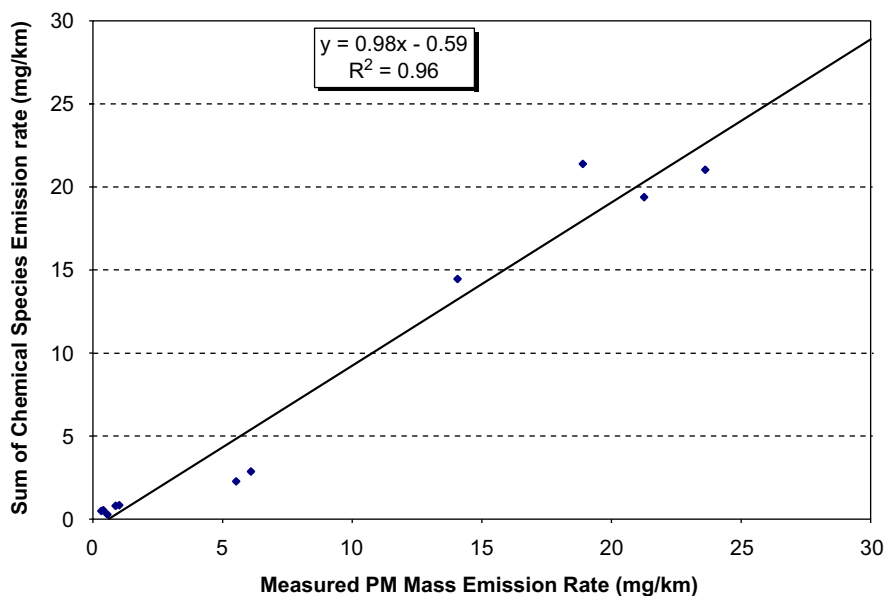Fig. 4. Regression of the sum of chemical species and the gravimetrically determined mass emission rates.

Table 5
DTT consumption rates (nmole min^{-1} km^{-1})

Vehicle and driving cycle	DTT rate of consumption (nmol min^{-1} km^{-1})	DTT rate of consumption (nmole min^{-1} μg^{-1} of PM mass emitted)
Diesel transient	0.88 ($\pm$0.2)	0.039 ($\pm$0.05)
Diesel steady state	0.48	0.034
Cat. DPF transient	0.11 ($\pm$0.02)	0.110 ($\pm$0.02)
Gasoline transient	0.16 ($\pm$0.03)	0.025 ($\pm$0.03)

gasoline vehicle due to the low-mass loading collected during these experiments. The diesel passenger car demonstrated the highest level of PM redox activity in each of its test configurations, with the highest PM redox activity found in the emission of the transient cycles $(0.88 \pm 0.2$ nmol DTT min^{-1} km^{-1}), followed by the steady-state configuration of that vehicle (0.48 nmol DTT min^{-1} km^{-1}). The lowest PM redox activity was associated with the emissions of the DPF-equipped diesel vehicle, the DTT consumption rate of which was roughly 1/8 of that of the conventional diesel car. Substantially lower redox activity was also observed for the PM emitted from the gasoline vehicle during its transient cycle. The average DTT consumption rate was roughly five- and three-fold lower than those of the diesel vehicle during transient and steady-state cycles, respectively. It is quite striking that the emissions of the DPF-equipped diesel vehicle induced nearly 30% less

redox activity than the gasoline vehicle, a result that illustrates the effectiveness of after-treatment technologies in reducing the toxicological potential of PM from diesel vehicles.

The degree of correlation between the DTT consumption rates and individual chemical species for each experiment is shown in Table 6. As with Table 4 above, the degree of correlation between individual species emission rates and DTT was also examined by transforming these data into their logarithms. Results from both correlation analyses are shown in Table 6. The highest correlations were observed between DTT consumption and species mostly found in the exhaust of the highest emitting diesel vehicle (Honda Accord), including EC, OC (especially for the log-transformed data), the light molecular weight PAH, Be, Li, Al, Ni, and Zn, for all of which the R^2 between DTT consumption and species emission rates exceeded 0.80. Fig. 5(A–D) shows the log–log relationships between emission

Table 6
Coefficients of statistical determination (R^2) between the emission factors of chemical PM constituents and the rate of consumption of DTT

Species	Arithmetic data	Log-transformed data
OC	0.65	0.80
EC	0.98	0.85
NAP	0.89	0.65
PHE	0.86	0.63
ANT	0.46	0.38
FLT	0.16	0.21
PYR	0.94	0.83
BAA	0.43	0.45
CRY	0.47	0.51
Li	0.96	0.82
Be	0.93	0.68
Na	0.80	0.58
Mg	0.00	0.06
Al	0.82	0.57
S	0.73	0.51
K	0.61	0.29
Ca	0.78	0.46
Ti	0.69	0.32
V	0.44	0.53
Cr	0.64	0.24
Mn	0.46	0.30
Fe	0.07	0.11
Ni	0.95	0.91
Cu	0.00	0.04
Zn	0.90	0.77
Ba	0.17	0.13
Pb	0.41	0.07

factors for the species listed in the previous paragraph versus their corresponding DTT consumption rates. The high degree of correlation between redox activity and these species persists even in the log-transformed data, although for most of them the R^2 decreases somewhat from the 0.80–0.95 to the 0.65–0.85 range. It should be emphasized here that the high correlation between redox activity and elements such as Li and Be may not necessarily reflect their redox activity, but rather the correlation of their concentration (as shown in Table 4) and redox-active species, such as EC, OC, light PAH, Zn, and Ni, whose activity has been demonstrated previously (Behndig et al., 2006; Cho et al., 2005). The degree of correlation actually increases substantially for OC (from 0.65 to 0.80) and for V (from 0.43 to 0.53) when the log-transformed emissions rates are considered. Here, we should point out some notable differences between the results of this study and those of McDonald et al. (2004), whose study only reported

significant associations between inflammatory markers and the concentrations of hopanes-steranes. It needs to be emphasized that these studies report different metrics of toxicity, but a comparison between the two reveals the difficulty in associating health effects with particular PM components. While PAHs and metals did not correlate with lung inflammation, certain PAHs and various metals correlated with the redox activity in the present study. Thus, establishing the metric of toxic response is as important as ascertaining its relation to individual PM chemical species.

While the high degree of association between DTT and certain PM species appears to be promising for predicting the PM toxicity of a given vehicle's exhaust based on its chemical composition, it must be reiterated that each species alone may not necessarily be responsible for the redox activity response. This point is further reinforced by noting that the reductions in DTT activity and the reductions in mass PM emission are non-linearly related, as evidenced by examining the normalized rate of DTT consumption per PM mass emitted, a metric of the PM intrinsic redox potential, shown in the last column of Table 5. While the PM mass emission rate from the DPF-equipped vehicle was on average approximately 25 times lower than that of the conventional diesel, the redox potential was only eight times lower, which makes the per mass PM redox potential of the DPF vehicle about 3 times higher, as listed in Table 5. Therefore, while particle reduction technologies effectively reduce the vast majority of both mass and number from vehicle emissions, the redox activity of PM in these emissions is not diminished at the same rate.

The most obvious difference in the chemical composition between the DPF-equipped vehicle and the rest of the vehicles tested is its very high OC mass fraction, accounting for roughly 60% of the total PM mass emitted during the transient cycle, compared to approximately 20% and 30% of the diesel and gasoline vehicles, respectively. The sum of the PAH measured accounts for a very small portion of the total OC in each vehicle, suggesting that there may be several other organic species in the exhaust that are potentially important from a toxicological perspective. More detailed organic speciation of the PM emitted by various vehicles was beyond the scope of the current study, but it could very well be the subject of future investigations, which could also examine the degree of
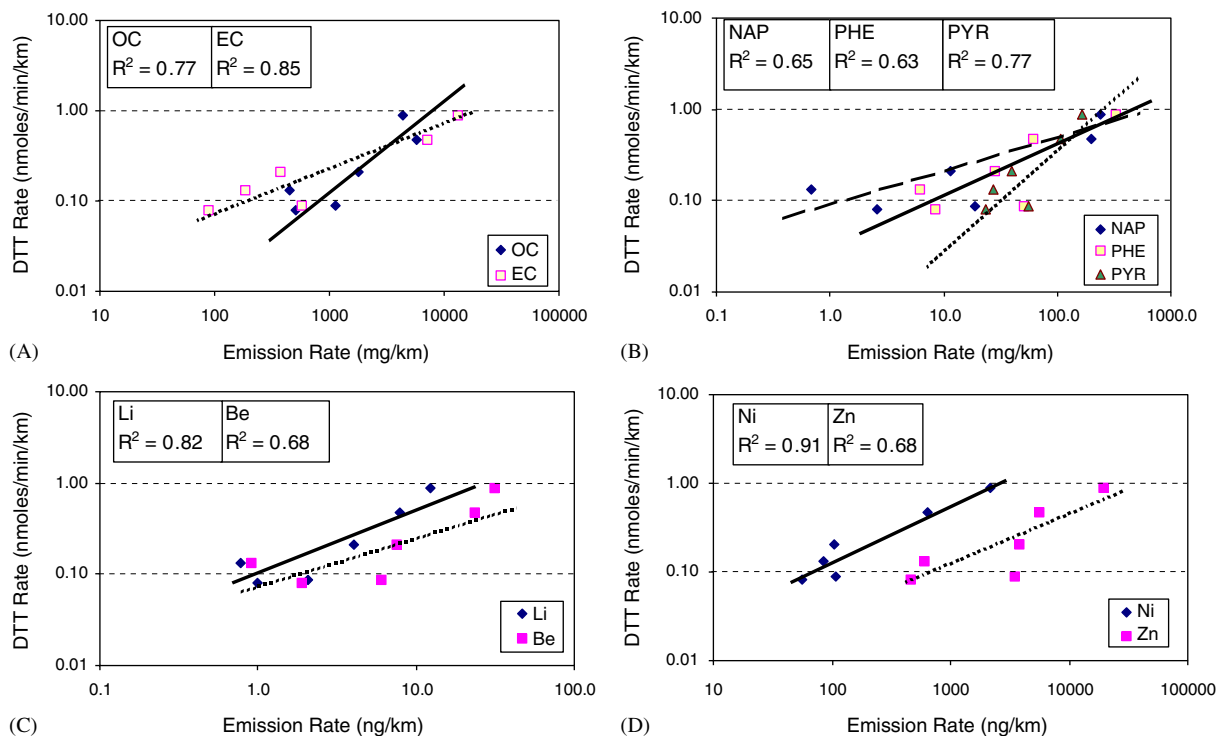
Fig. 5. Linear relationships between emission factors for selected species listed versus their corresponding DTT consumption rates; (A) elemental and organic carbon; (B) pyrene, naphthalene, and phenanthrene; (C) lithium and beryllium; (D) nickel and zinc.

association between these species and additional toxicological bioassays. As we stated earlier in our Introduction, our study was by no means comprehensive, and was restricted to few vehicles and driving configurations that are thought to be representative of the current light duty diesel and gasoline fleet of Europe. Nevertheless, there was remarkable consistency in the reported associations between some PM-bound chemical species and the DTT-based redox assay, despite the rather limited number of experiments. We intend to investigate the relationship between PM emitted from other types of vehicles, including heavy-duty trucks, with and without after-treatment control technologies, as well as compressed natural gas (CNG) buses, and several additional bioassays that are indicative of oxidative stress in future efforts.

4. Summary and conclusions

This study reports relationships between physical and chemical characteristics of PM and redox activity of diesel and gasoline particulate emissions from passenger cars typically in use in Europe. Results showed a high degree of correlation between

redox activity of PM and several PM species, including EC, OC, low molecular weight PAHs, and several trace elements, which are species mostly found in the exhaust of the highest emitting diesel vehicle tested. The reduction in PM mass or number emission factors resulting from the various engine configurations, fuel types and/or after-treatment technologies, however, was non-linearly related to the decrease in overall PM redox activity. While the PM mass emission rate from the DPF-equipped vehicle was on average approximately 25 times lower than that of the conventional diesel, the redox potential was only 8 times lower. Therefore, the high degree of association between DTT and certain PM species shows promise for predicting PM toxicity of a given vehicle's exhaust based on its chemical composition, bearing in mind each species may not necessarily be solely responsible for the redox activity response. Thus, a strategy aimed at protecting public health and welfare by reducing total vehicle mass and number emissions may not fully achieve the desired goal of preventing the health consequences of PM exposure. Further, study of the chemical composition and interactions between various chemical species may yield greater

insights into the toxicity of the PM content of vehicle exhaust.

Acknowledgments

References

Adler, K.B., Fischer, B.M., Wright, D.T., Cohn, L.A., Becker, S., 1994. Interactions between respiratory epithelial-cells and cytokines—relationships to lung inflammation. Cells and Cytokines in Lung Inflammation 725, 128–145.

Andre, M., 2004. The artemis European driving cycles for measuring car pollutant emissions. Science of the Total Environment 334–35, 73–84.

Arhami, M., Kuhn, T., Fine, P.M., Delfino, R.J., Sioutas, C., 2006. Effects of sampling artifacts and operating parameters on the performance of a semicontinuous particulate elemental carbon/organic carbon monitor. Environmental Science and Technology 40 (3), 945–954.

Baulig, A., et al., 2003. Involvement of reactive oxygen species in the metabolic pathways triggered by diesel exhaust particles in human airway epithelial cells. American Journal of Physiology—Lung Cellular and Molecular Physiology 285 (3), L671–L679.

Behndig, A.F., et al., 2006. Airway antioxidant and inflammatory responses to diesel exhaust exposure in healthy humans. European Respiratory Journal 27 (2), 359–365.

Birch, M.E., Cary, R.A., 1996. Elemental carbon-based method for monitoring occupational exposures to particulate diesel exhaust. Aerosol Science and Technology 25 (3), 221–241.

Burtscher, H., 2005. Physical characterization of particulate emissions from diesel engines: a review. Journal of Aerosol Science 36 (7), 896–932.

Cho, A.K., et al., 2005. Redox activity of airborne particulate matter at different sites in the Los Angeles Basin. Environmental Research 99 (1), 40–47.

Cyrys, J., et al., 2003. Elemental composition and sources of fine and ultrafine ambient particles in Erfurt, Germany. Science of the Total Environment 305 (1–3), 143–156.

Dekati, L., 2001. Sampling automotive exhaust with a thermodenuder. Dekati Ltd., Technical Note.

Dellinger, B., et al., 2001. Role of free radicals in the toxicity of airborne fine particulate matter. Chemical Research in Toxicology 14 (10), 1371–1377.

Dockery, D.W., et al., 1993. An association between air-pollution and mortality in 6 United-States cities. New England Journal of Medicine 329 (24), 1753–1759.

Donaldson, K., Stone, V., Seaton, A., MacNee, W., 2001. Ambient particle inhalation and the cardiovascular system: potential mechanisms. Environmental Health Perspectives 109, 523–527.

Durbin, T.D., Collins, J.R., Norbeck, J.M., Smith, M.R., 2000. Effects of biodiesel, biodiesel blends, and a synthetic diesel on emissions from light heavy-duty vehicles. Environmental Science and Technology 34 (3), 349–355.

Eatough, D.J., Eatough, D.A., Lewis, L., Lewis, E.A., 1996. Fine particulate chemical composition and light extinction at Canyonlands National Park using organic particulate material concentrations obtained with a multisystem, multichannel diffusion denuder sampler. Journal of Geophysical Research-Atmospheres 101 (D14), 19515–19531.

Eiguren-Fernandez, A., Miguel, A.H., 2003. Determination of semivolatile and particulate polycyclic aromatic hydrocarbons in srm 1649a and PM$_{2.5}$ samples by HPLC-fluorescence. Polycyclic Aromatic Compounds 23 (2), 193–205.

Geller, M.D., Sardar, S.B., Phuleria, H., Fine, P.N., Sioutas, C., 2005. Measurements of particle number and mass concentrations and size distributions in a tunnel environment. Environmental Science and Technology 39 (22), 8653–8663.

Geller, M.D., Biswas, S., Sioutas, C., 2006. Determination of particle effective density in urban environments with an Aerosol Particle Mass Analyzer and Differential Mobility Analyzer. Aerosol Science and Technology 40, 709–723.

Giechaskiel, B., Ntziachristos, L., Samaras, Z., 2004. Calibration and modelling of ejector dilutors for automotive exhaust sampling. Measurement Science and Technology 15 (10), 2199–2206.

Gross, D.S., et al., 2000. Single particle characterization of automobile and diesel truck emissions in the Caldecott Tunnel. Aerosol Science and Technology 32 (2), 152–163.

Jang, M.S., Kamens, R.M., 2001. Characterization of secondary aerosol from the photooxidation of toluene in the presence of NO$_x$ and 1-propene. Environmental Science and Technology 35 (18), 3626–3639.

Kirchstetter, T.W., Corrigan, C.E., Novakov, T., 2001. Laboratory and field investigation of the adsorption of gaseous organic compounds onto quartz filters. Atmospheric Environment 35 (9), 1663–1671.

Kittelson, D.B., 1998. Engines and nanoparticles: a review. Journal of Aerosol Science 29 (5–6), 575–588.

Lanki, T., et al., 2006. Can we identify sources of fine particles responsible for exercise-induced ischemia on days with elevated air pollution? The ULTRA study. Environmental Health Perspectives 114, 655–660.

Li, N., et al., 2001. Use of a stratified oxidative stress model to study ambient and diesel particle effects. Free Radical Biology and Medicine 31, S117.

Li, N., et al., 2003. Ultrafine particulate pollutants induce oxidative stress and mitochondrial damage. Environmental Health Perspectives 111 (4), 455–460.

Lough, G.C., et al., 2005. Emissions of metals associated with motor vehicle roadways. Environmental Science and Technology 39 (3), 826–836.

Maejima, K., et al., 2001. Effects of the inhalation of diesel exhaust, Kanto loam dust, or diesel exhaust without particles on immune responses in mice exposed to Japanese cedar (*Cryptomeria japonica*) pollen. Inhalation Toxicology 13 (11), 1047–1063.

Marr, L.C., et al., 1999. Characterization of polycyclic aromatic hydrocarbons in motor vehicle fuels and exhaust emissions. Environmental Science and Technology 33 (18), 3091–3099.

Mayer, A., Matter, U., Scheidegger, G., Czerwinski, J., Wyser, M., Kieser, D., Weidhofer, J., 1999. Particulate traps for retro-fitting construction site engines VERT: final measurement and implementation. 1999-01-0116, SAE.

McDonald, J.D., et al., 2004. Relationship between composition and toxicity of motor vehicle emission samples. Environmental Health Perspectives 112 (15), 1527–1538.

Miguel, A.H., Kirchstetter, T.W., Harley, R.A., Hering, S.V., 1998. On-road emissions of particulate polycyclic aromatic hydrocarbons and black carbon from gasoline and diesel vehicles. Environmental Science and Technology 32 (4), 450–455.

Ntziachristos, L., Giechaskiel, B., Ristimaki, J., Keskinen, J., 2004. Use of a corona charger for the characterisation of automotive exhaust aerosol. Journal of Aerosol Science 35 (8), 943–963.

Pierson, W.R., Brachaczek, W.W., 1983. Particulate matter associated with vehicles on the road .2. Aerosol Science and Technology 2 (1), 1–40.

Pope, C.A., Dockery, D.W., Schwartz, J., 1995. Review of epidemiological evidence of health-effects of particulate air-pollution. Inhalation Toxicology 7 (1), 1–18.

Sakurai, H., et al., 2003. Size-dependent mixing characteristics of volatile and nonvolatile components in diesel exhaust aerosols. Environmental Science and Technology 37 (24), 5487–5495.

Schafer, M., Schafer, C., Ewald, N., Piper, H.M., Noll, T., 2003. Role of redox signaling in the autonomous proliferative response of endothelial cells to hypoxia. Circulation Research 92 (9), 1010–1015.

Seagrave, J.C., et al., 2001. Comparative acute toxicities of particulate matter and semi-volatile organic compound fractions of traffic tunnel air. Toxicologist 60, 192.

Seagrave, J., et al., 2002. Mutagenicity and in vivo toxicity of combined particulate and semivolatile organic fractions of gasoline and diesel engine emissions. Toxicological Sciences 70 (2), 212–226.

Seagrave, J., Mauderly, J.L., Seilkop, S.K., 2003. In vitro relative toxicity screening of combined particulate and semivolatile organic fractions of gasoline and diesel engine emissions.

Journal of Toxicology and Environmental Health-Part A 66 (12), 1113–1132.

Shi, J.P., Harrison, R.M., 1999. Investigation of ultrafine particle formation during diesel exhaust dilution. Environmental Science and Technology 33 (21), 3730–3736.

Sigaud, S., Evelson, P., Gonzalez-Flecha, B., 2005. H_2O_2-induced proliferation of primary alveolar epithelial cells is mediated by MAP kinases. Antioxidants and Redox Signaling 7 (1–2), 6–13.

Solomon, P.A., Fall, T., Salmon, L., Cass, G.R., Gray, H.A., Davidson, A., 1989. Chemical characteristics of PM_{10} aerosols collected in the Los Angeles area. Journal of Air Pollution Control Association 39, 2154–2163.

Squadrito, G.L., Cueto, R., Dellinger, B., Pryor, W.A., 2001. Quinoid redox cycling as a mechanism for sustained free radical generation by inhaled airborne particulate matter. Free Radical Biology and Medicine 31 (9), 1132–1138.

Su, D.S., et al., 2004. Fullerene-like soot from EuroIV diesel engine: consequences for catalytic automotive pollution control. Topics in Catalysis 30–31 (1–4), 241–245.

Subramanian, R., Khlystov, A.Y., Cabada, J.C., Robinson, A.L., 2004. Positive and negative artifacts in particulate organic carbon measurements with denuded and undenuded sampler configurations. Aerosol Science and Technology 38, 27–48.

Turpin, B.J., Huntzicker, J.J., Hering, S.V., 1994. Investigation of organic aerosol sampling artifacts in the Los-Angeles basin. Atmospheric Environment 28 (19), 3061–3071.

Vaaraslahti, K., Virtanen, A., Ristimaki, J., Keskinen, J., 2004. Nucleation mode formation in heavy-duty diesel exhaust with and without a particulate filter. Environmental Science and Technology 38 (18), 4884–4890.

Venkataraman, C., Lyons, J.M., Friedlander, S.K., 1994. Size distributions of polycyclic aromatic-hydrocarbons and elemental carbon. 1. Sampling, measurement methods, and source characterization. Environmental Science and Technology 28 (4), 555–562.

Veronesi, B., Oortgiesen, M., Carter, J.D., Devlin, R.B., 1999. Particulate matter initiates inflammatory cytokine release by activation of capsaicin and acid receptors in a human bronchial epithelial cell line. Toxicology and Applied Pharmacology 154 (1), 106–115.

Virtanen, A., Ristimaki, J., Keskinen, J., 2004. Method for measuring effective density and fractal dimension of aerosol agglomerates. Aerosol Science and Technology 38 (5), 437–446.

Vogl, G., Elstner, E.F., 1989. Diesel soot particles catalyze the production of oxy-radicals. Toxicology Letters 47 (1), 17–23.

Wang, Y.F., et al., 2003. Emissions of fuel metals content from a diesel vehicle engine. Atmospheric Environment 37 (33), 4637–4643.

Zielinska, B., et al., 2004a. Phase and size distribution of polycyclic aromatic hydrocarbons in diesel and gasoline vehicle emissions. Environmental Science and Technology 38 (9), 2557–2567.

Zielinska, B., Sagebiel, J., McDonald, J.D., Whitney, K., Lawson, D.R., 2004b. Emission rates and comparative chemical composition from selected in-use diesel and gasoline-fueled vehicles. Journal of the Air and Waste Management Association 54 (9), 1138–1150.